Atmos. Chem. Phys. Discuss., doi:10.5194/acp-2015-904, 2016
Manuscript under review for journal Atmos. Chem. Phys.
Published: 26 January 2016

Atmospheric Chemistry and Physics Discussions

Polarization properties of aerosol particles over western Japan: classification, seasonal variation, and implications for air quality

X.L. Pan[1], I. Uno[1], Y. Hara[1], K. Osada[2], S. Yamamoto[3], Z. Wang[6], N. Sugimoto[4], H. Kobayashi[5] and Z.F. Wang[6]

[1] Research Institute for Applied Mechanics, Kyushu University, Fukuoka, Japan

[2] Graduate School of Environmental Studies, Nagoya University, Nagoya, Japan

[3] Fukuoka Institute of Health and Environmental Sciences, Fukuoka, Japan

[4] National Institute for Environmental Studies, Ibaraki, Japan

[5] University of Yamanashi, Yamanashi, Japan

[6] Institute of Atmospheric Physics, Chinese Academy of Sciences, Beijing, China

Corresponding author: X.L. Pan (xlpanelf@riam.kyushu-u.ac.jp)

Abstract

Ground-based observations of the polarization properties of aerosol particles using a polarization optical particle counter (POPC) were performed from October 2013 to January 2015 at a suburban site in the Kyushu area of Japan. By conducting an analysis of online measurements of aerosol composition, we investigated size-dependent polarization characteristics for three typical aerosol types (anthropogenic pollutants, dust, and sea salt). We found that, for supermicron particles, its depolarization ratio (DR, the fraction of s-polarized signal in the total backward light scattering signal) generally increased with the particle size, and a threshold value of 0.1 could be used to identify their sphericity. In summer, air pollution was less serious, and the DR of aerosol particles was relatively small due to the influence of spherical sea salt particles in high humidity conditions. This study indicated that air masses were transported across the Asian continent and contained not only anthropogenic pollutants, but also large amounts of non-spherical particles (i.e., dust), which could impact on the air quality in western Japan, especially in winter and spring. The variation of number fraction of spherical particles did not correlate with relative humidity averaged along the trajectories of air parcels, indicating the coexistence of hydrophobic substances (e.g., mineral dust and organics), although the sulfate and nitrate mass concentrations were high.

Atmos. Chem. Phys. Discuss., doi:10.5194/acp-2015-904, 2016
Manuscript under review for journal Atmos. Chem. Phys.
Published: 26 January 2016

Atmospheric Chemistry and Physics Discussions

1. Introduction

The East Asian region is characterized by serious regional anthropogenic pollution, due to the mass consumption of fossil fuel in China (Kurokawa *et al.,* 2013). This region is also influenced by sporadic occurrences of dust plumes from the Taklimakan/Gobi desert (Uno *et al.,* 2009, Yumimoto *et al.,* 2009). The environmental/climate effects of these anthropogenic and mineral dust aerosols are notably different because of their distinct chemical and physical properties, size distributions, and lifetimes in the troposphere (Pan *et al.,* 2009). Dust aerosols can trap substantial amounts of pollutants (e.g., nitrate), forming a so-called "polluted dust" when they are transported through the planetary boundary layer (PBL) of polluted areas (Wang *et al.,* 2002, Zhang *et al.,* 2005, Zhang *et al.,* 2006). As a consequence, there is substantial variability in their resulting hygroscopic properties, which contributes to considerable uncertainty in predicting their climate effects with models. The light polarization property of a particle is a good proxy indicator of its sphericity/non-sphericity. As such, remote sensing with ground-based Lidar and Cloud-Aerosol Lidar with Orthogonal Polarization (CALIOP) has been used for the last decade to provide valuable information regarding the vertical and horizontal distribution of pollutants and dust particles in the atmosphere (Shimizu *et al.,* 2004, Winker *et al.,* 2009, Sugimoto *et al.,* 2015). The Asian Dust and aerosol lidar observation Network (AD-Net) has also been established to observe the temporal and spatial characteristics of dust and pollutant particles using a polarization-sensitive (532 nm) two-wavelength (1064 and 532 nm) lidar (Sugimoto and Huang 2014). They can be used to investigate the mixing state of dust particles because the data points of pure dust particles are normally in the upper-right portion of a depolarization versus backscattering ratio (1064nm/532 nm) plot, clearly separate from the data points of pollutant aerosols (in the lower-left portion), with data to the right side of the line connecting the two data clusters reflecting the variation of the mixing state of particles (Sugimoto *et al.,* 2002). Theoretically, the particles with a smaller depolarization ratio (DR, the fraction of *s*-polarized to the total backward scattering, [$S/(S+P)$]) and larger backscattering color ratio may be related to internally mixed Asian dusts; however, this cannot be confidently concluded because the external mixture of dust and large spherical particles (e.g., sea salt) has a similar pattern on the basis of volume backscattering measurements by lidar (Sugimoto *et al.,* 2015).

Recently, a bench-top optical particle counter equipped with a depolarization module was developed. The major advantage of this instrument is its ability to depict the size-resolved polarization of particles (Kobayashi *et al.,* 2014), providing the potential to quantitatively investigate the evolution of the mixing of dust particles during their transport. A study in Seoul (Longitude: 128.95E, Latitude: 37.46N, 116 m a.s.l.) reported the internal mixing of

Atmos. Chem. Phys. Discuss., doi:10.5194/acp-2015-904, 2016
Manuscript under review for journal Atmos. Chem. Phys.
Published: 26 January 2016

Atmospheric Chemistry and Physics Discussions

Asian dust with anthropogenic pollutants on the basis of an evident decrease in the backscattering DR of all particles during a polluted dust episode (Sugimoto *et al.*, 2015). The observation (Pan *et al.*, 2015) of a 7-day dust event in Kyushu in 2014 found that the size-dependent polarization property of particles varied significantly throughout the dust event, and the decrease in the DR of supermicron particles was mostly due to an increase in the coarse mode nitrate concentration. This phenomenon was verified by an off-line analysis with transmission electron microscopy (Li and Shao 2009, Li *et al.,* 2011) and a model simulation, which highlighted the direct absorption of nitric acid gas by the dust surface, and/or the volatilization of ammonium nitrate particulate as well as the resulting transfer of nitrate to the dust due to heterogeneous reactions during transport (Allen *et al.,* 2015).

To determine the mixing state of dust particles outflowing from the Asian continent, a long-term field observation was performed at a suburban site (Longitude: 130.47°E, Latitude: 33.52°N) in Fukuoka, on the westernmost edge of Japan, beginning in October 2013. The geographic location of the observation site is shown in Figure 1. This location is subject to long-range transport (LRT) of both anthropogenic pollutions and dust plumes from the Asian continent in spring and autumn. Although local emissions (e.g., NO_x) contribute to the nitrate mass, LRT is largely responsible for the buildup of $PM_{2.5}$ (particulate matter with a diameter less than or equal to 2.5 μm) in this city (Kaneyasu *et al.,* 2014), particularly during the late winter-spring period. In this study, size-dependent polarization characteristics for single particle were continuously measured by a polarization optical particle counter (POPC), and three common aerosol types (anthropogenic pollutants, dust, and sea salt) were classified, together with an analysis of some key pollutant parameters (sulfate, nitrate, particulate acidity, etc.). The contributions of different aerosol types to ambient aerosol concentrations were discussed. The sphericity/non-sphericity of aerosols from different origins, their relative humidity (RH) dependence, and corresponding impacts on the local air quality in Fukuoka city were investigated using a combined ensemble backward trajectory analysis.

2. Measurements

The light polarization properties of atmospheric aerosol particles (with particle diameter, Dp < 10 μm) were measured using a newly developed POPC (YGK Corp., Yamanashi, Japan) at the top of a two-story building at Kyushu University (Longitude: 130.5°E, Latitude: 33.5°N). We installed a 3 m-long vertical stainless steel tube through the roof of the building, and ambient air was drawn into the room with a laminar flow rate of 13 L/min. The loss of coarse mode particles (Dp > 2.5 μm) due to gravity settling was negligible. The POPC uses a 780 nm

Atmos. Chem. Phys. Discuss., doi:10.5194/acp-2015-904, 2016
Manuscript under review for journal Atmos. Chem. Phys.
Published: 26 January 2016

Atmospheric Chemistry and Physics Discussions

linearly polarized laser source, and measures both forward scattering and backward scattering intensities at 60 degrees and 120 degrees, relative to the direction of incident light. A detailed description of the instrumentation is shown in Figure 2. The polarization direction of the incident laser is parallel to the plane of the scattering angle, and the acceptance angle for the polarization detector is 45 degrees. This configuration was optimized to reduce uncertainties in optical measurements (Kobayashi *et al.,* 2014). The size of particles is determined from the forward scattering intensity, and two polarized compounds (*s*-polarized/*p*-polarized, polarization direction perpendicular/parallel to the plane of the scattering angle) of backward scattering are measured simultaneously. In practice, the DR is a good indicator of particle sphericity because the direction of polarization of scattered light for spherical particles is identical to that of the incident light, while this is not the case for non-spherical particles (e.g., dust). The DR thresholds for determining the sphericity/non-sphericity of particles are not uniform for different optical instrumentations. For example, lidar observations classify aerosols on the basis of an empirically determined aerosol back-scattering DR (δ_a = S/P), and the values of δ_a <0.02 and δ_a >0.35 (DR = 0.003, 0.26, respectively in this context) are regarded as the thresholds for pure spherical and non-spherical dust particles (Shimizu *et al.,* 2004). Regarding the use of a POPC, Kobayashi et al. (2014) proposed a threshold of DR >0.2 as being "non-spherical" for supermicron particles (e.g., dust) according to the number concentration of particles measured at Fukuoka University (Longitude: 33.5°N, Latitude: 130.36°E).

In this study, mass concentrations of particulate matter (PM), sulfate, nitrate, and water-soluble organic compounds in both the fine (Dp <2.5 μm) and coarse mode were measured using a continuous dichotomous Aerosol Chemical Speciation Analyzer (ACSA-12, KIMOTO electric Co. Ltd, Osaka, Japan) at 1 h intervals. The mass concentration of PM and sulfate ion were determined using the beta-ray absorption method and the $BaSO_4$-based turbidimetric method, after the addition of $BaCl_2$ dissolved in polyvinylpyrrolidone solution. The mass concentrations of nitrate ion and water-soluble organic compounds were determined with an ultraviolet absorption-photometric method. The details of the ACSA instrument have been published elsewhere (Kimoto *et al.,* 2013).

3. Results

3.1 Temporal variation

The daily-averaged volume concentrations in different aerosol size bins at the observation site are shown in Figure 3. In general, the volume concentrations of ambient particles had two

Atmos. Chem. Phys. Discuss., doi:10.5194/acp-2015-904, 2016
Manuscript under review for journal Atmos. Chem. Phys.
Published: 26 January 2016

Atmospheric Chemistry and Physics Discussions

pronounced peaks in the submicron and/or coarse mode size ranges, particularly in spring and winter. The peak in the submicron range was related to anthropogenic pollution (marked as "P" in Figure 3a), while the coarse mode peak (4–8 μm) was attributed to mineral dust (marked as "D" in Figure 3a). The two peaks occurred concurrently or sequentially as a result of different prominent outflow patterns. Itahashi *et al.*(2010) found that dust and pollution were trapped and well mixed within the PBL (referred to as "mixed type" and marked as "M" in Figure 3a), when dust events broke out "behind a cold front," and were characterized by strong stratification. In summer, the volume concentration of particles in both fine and coarse modes decreased significantly because the air masses mostly originated from the western Pacific Ocean where anthropogenic emissions were limited. Wet scavenging processes were significant in the summertime of Kyushu. The DR value of particles at each size range as a function of time in 2014 is also shown in Figures 3b and 3d. Because DR value of any size range particles was always characterized by a skewness of the distribution, we use a mode DR (MDR) value to represent the their typical depolarization property. In general, MDR value increased evidently with increase of their size. Anthropogenic pollutants could also impact MDR values of large particles. A week-long dust event at the end of May 2014 showed that MDR of supermicron particles decreased evidently due to intricate mixing with water-soluble pollutants (Pan *et al.,* 2015).

3.2 Size distribution

The overall volume size distribution and MDR of aerosol particles in Kyushu displayed clear seasonal variation, as demonstrated in Figure 4. In spring (MAM), the volume size distribution of particles had a broad peak in the coarse mode due to the impact of frequent outbreaks and transport of Asian dust (Figure 4a). Aerosol particles with Dp < 2.5 μm had a small MDR (~0.02; Figures 4b, 4d, 4f and 4h). The MDR of coarse mode particles was larger than 0.1, and displayed a clear increasing trend with increasing particle size. In summer (JJA), the volume concentration of particles did not change with size (Figure 4c). Remarkably, aerosol particles in the coarse mode also had a relatively small MDR (<0.1, Figure 4d). This was mostly due to air masses that originated from clean marine regions and consisted of large amounts of sea salt aerosols, which tend to be spherical under high-humidity conditions. In autumn (SON) and winter (DJF), there was a prominent mode in the submicron range, indicating the predominance of anthropogenic pollutants. The MDR value increased with an increase in particle size because of the presence of non-spherical particles, especially when the air mass originated from the Asian continent.

Atmos. Chem. Phys. Discuss., doi:10.5194/acp-2015-904, 2016
Manuscript under review for journal Atmos. Chem. Phys.
Published: 26 January 2016

Atmospheric Chemistry and Physics Discussions

The slope of the DR as a function of particle size between 4 and 9 μm (referred to as "SlopeDR") included some basic information regarding the coarse mode particles, because the mixing of dust particles with pollutants may result in an increase in the imaginary part of their refractive index, resulting in a decrease of the DR at the 120° backscattering angle (Dubovik *et al.,* 2006). We found that the SlopeDR was 0.8 in spring, highest among those in autumn (0.5) and winter (0.6). The most likely explanation for this was that the air masses in spring, which originated from the interior of the Asian continent with high wind speeds, contained many more dust particles than in the other seasons. Another possibility is that dust particles in autumn and winter underwent complex mixing processes because of stagnancy in marine areas (Tobo *et al.,* 2010). The SlopeDR in summer was lower than 0.1 due to the presence of deliquescent sea salt aerosols under high RH condition. In autumn, the DR value of coarse mode particles varied significantly, indicating that they had different origins.

4 Discussion

4.1 Size polarization properties for aerosol classification

We selected three special cases dominated significantly by distinct aerosols types, which were based on the mass concentrations of $PM_{2.5}$ and $PM_{2.5\text{-}10}$ (2.5 μm < Dp < 10 μm), and SO_4^{2-} ion in the fine mode (fSO_4^{2-}), and NO_3^- ions in both the fine (fNO_3^-) and coarse mode (cNO_3^-), as shown in Table 1. During pollution episodes, the mass concentration of $PM_{2.5}$ was 63.4 μg/m^3, which was about five times higher than the $PM_{2.5\text{-}10}$ concentrations (12.9 μg/m^3). The SO_4^{2-} and fNO_3^- ions accounted for 50% of the total $PM_{2.5}$ mass. During dust episodes, the mass concentrations of $PM_{2.5}$ and $PM_{2.5\text{-}10}$ were 27.5 and 62.9 μg/m^3, respectively, with minimal contributions from anthropogenic pollutants to the $PM_{2.5}$ mass (SO_4^{2-} : 2.7 μg/m^3; fNO_3^- : 1.4 μg/m^3). Because we did not measure sodium or chloride ions, a quantitative determination of the influence of sea salt was difficult; however, we could reasonably assume that during the typhoon period, sea salt aerosol was dominant. Detailed information regarding the trajectory of the two typhoon cases (No.18 PHANFONE and No.19 VONGFONG) during the study period is described in the Japan Meteorological Agency webpage (http://www.data.jma.go.jp/fcd/yoho/typhoon/route_map/index.html). The mass concentrations of $PM_{2.5}$, $PM_{2.5\text{-}10}$, SO_4^{2-}, and fNO_3^- were minimal during the typhoon period (13 hours in total), with mean values of 6.6, 9.7, 1.3, and 0.5 μg/m^3, respectively.

To identify the polarization characteristics for the different aerosol types, a DR-Dp-volume plot of the particles during specific periods was produced (Figure 5). We divided the DR-Dp-volume image into four areas. Anthropogenic pollutants were mostly in the submicron range,

Atmos. Chem. Phys. Discuss., doi:10.5194/acp-2015-904, 2016
Manuscript under review for journal Atmos. Chem. Phys.
Published: 26 January 2016

Atmospheric Chemistry and Physics Discussions

with DR values <0.2 (marked as region A1, as shown in Figure 5a). Mineral dust had a larger diameter (Dp >3 μm) and a non-spherical morphology associated with larger DR values (MDR = 0.4; region A2, as shown in Figure 5b). Sea salt aerosols were in the supermicron range, with DR values <0.1 (marked as region A3, as shown in Figure 5c). During the typhoon period (RH = 76% on average), we considered the sea salt particles to be spherical because sea salt is deliquescent when RH >75% (Wise *et al.,* 2007). Based on this information, we proposed a DR threshold value of 0.1 to distinguish between spherical and non-spherical particles in the supermicron size range. This criterion was consistent with the theoretical Mie-scattering calculation and classification in the literature (Kobayashi *et al.,* 2014). The sphericity/non-sphericity of submicron particles with DR >0.2 was not considered because of the low volume concentration. With regard to A1, we cannot be specific about the sphericity/non-sphericity of the particles, because the morphology of anthropogenic particles is extremely variable, and depends on the mass fractions of carbonaceous matter and water-soluble inorganics, as well as meteorological conditions (e.g., RH), the mixing state, and the degree of atmospheric aging (Li *et al.,* 2011, Fu *et al.,* 2012). Additionally, the *s*-polarized backscattering of submicron particles decreased significantly with a decrease in their size on the basis of theoretical simulations, even for non-spherical particles (Sugimoto *et al.,* 2015).

4.2 Contributions of different aerosol types to local air quality

Using the criteria suggested from specific periods, the impacts of different aerosol types on air quality in western Japan were considered. Here, the DR-Dp-volume plot was made at 1-day intervals (0000 JST – 2300 JST), and the dominant mode was determined. Period when only one volume mode in A1, A2 or A3 was regarded as being pollution, mineral dust, or sea salt dominated, respectively. Periods when three distinct modes occurred simultaneously in A1, A2 and A3 were considered to represent a "mixed type," as shown in Figure 5d. Cases when two volume modes appeared in both A1 and A3 or in both A2 and A3 were regarded as pollution-dominant or dust-dominant periods, respectively.

Monthly-averaged mass concentrations of $PM_{2.5}$ and $PM_{2.5-10}$ are shown in Figure 6a. In general, ambient $PM_{2.5}$ levels displayed a clear winter-spring high and summer low. In contrast, the mass of $PM_{2.5-10}$ had a pronounced peak in May, reflecting frequent dust events. The number of days that the daily-averaged mass concentration of $PM_{2.5}$ exceeded the National Ambient Air Quality Standard (NAAQS) of Japan (35 μg/m^3) was highest in spring (Figure 6b). During May 2014, the NAAQS was exceeded on 12 days; mineral dust was responsible for about 70% of these substandard days, followed by other mixed pollution types

Atmos. Chem. Phys. Discuss., doi:10.5194/acp-2015-904, 2016
Manuscript under review for journal Atmos. Chem. Phys.
Published: 26 January 2016

Atmospheric Chemistry and Physics Discussions

(20%). In April 2014, no dust event was observed because of the weak cold air over the Inner Mongolian region, which was unusual compared with past observations. In March 2014, mixed pollution and dust dominated, accounting for 60% and 30% of substandard days, respectively (Figure 6c). Mixed pollution types clearly made the largest contribution to the number of days with substandard local air quality in the winter, and the smallest contribution in summer and autumn. This was because air masses passed through arid/semi-arid polluted regions in the Asian continent in winter, and dust particles and anthropogenic pollutants mixed during LRT. In summer 2014, only a few substandard air quality days were related to anthropogenic pollution (Figure 6b).

4.3 Polarization properties of aerosols from different origins

The DR-Dp-volume plots of aerosol particles from different origins were evaluated in combination with a backward trajectory analysis. The footprint regions for anthropogenic pollutants were determined based on ensemble simulations of 5-day backward trajectories of air parcels using the Hybrid Single Particle Lagrangian Integrated Trajectory (HYSPLIT) model (v4.9; available at http://ready.arl.noaa.gov/HYSPLIT.php), offsetting the release point by a meteorological grid point in the horizontal and 0.01 sigma units in the vertical. We divided the region of interest into four sub-regions, where the emission flux of anthropogenic pollutants and their corresponding aerosol types were different. When the air mass came from Region I (Figure 7a), which mostly covered the Sea of Japan and the Japanese landmass, the DR-Dp-volume plot had one predominant peak at MDR = 0.05 and Dp = 1.8 μm (Figure 7b). This suggested that spherical particles (e.g., sea salt) in the fine mode comprised most of the aerosol. Only 2% of this period was found to have substandard air quality. When the air mass came from Region II (covering the polluted region of North China and the Korean Peninsula, Figure 7c), the volume concentrations of particles in all size bins increased significantly, and the volume size distributions of particles had three distinct modes at Dp = 0.7 μm (MDR = 0.1), Dp = 1.9 μm (MDR = 0.08, and Dp = 5 μm (MDR = 0.35) (Figure 7d). The volume peaks in the submicron and coarse modes could be attributed to LRT of anthropogenic pollutants and mineral dust. The volume peak of particles at Dp = 1.9 μm (as shown by the black arrow in Figure 7d) indicated that there was a large fraction of non-spherical particles, in light of their large MDR values (from 0.08 up to 0.4), in contrast to the particles from Region I. We surmised that these particles were a mixture of both anthropogenic and dust particles. This was supported by our observations during a dust episode, which demonstrated that the DR values of supermicron dust particles were reduced when mixed with anthropogenic pollutants (Pan *et al.,* 2015). We found that 32% of the days, dominated by

Atmos. Chem. Phys. Discuss., doi:10.5194/acp-2015-904, 2016
Manuscript under review for journal Atmos. Chem. Phys.
Published: 26 January 2016

Atmospheric Chemistry and Physics Discussions

northwesterly winds, were substandard, i.e., anthropogenic pollutant, dust, and mixed particle types contributed to 13%, 8%, and 11% of particles, respectively. When air masses came from Region III (East China Sea, Figure 7e), 92% of these days met the NAAQS for Japan, and substandard days were mostly related to anthropogenic pollution (9%). The MDR (0.03) for supermicron particles was very small (Figure 7f), indicating a high degree of sphericity. Air masses from Region VI (western Pacific Ocean, Figure 7g) also contained a large volume fraction of supermicron particles, with small MDR values (~0.03). We found that substandard air quality days (16% of all days), when air masses came from Region VI, were more frequent than for Region III, reflecting the mixing of maritime air with local anthropogenic emissions over the western part of Japan (Figure 7g).

4.4 Fraction of spherical particles as a function of RH

As mentioned in previous studies (Koehler *et al.,* 2009, Sullivan *et al.,* 2009), the more dust particles become involved in chemical mixing, the more easily they become hydrophilic and are incorporated into cloud processes, which results in complicated climate effects. Here, the hygroscopicity of aerosol particles from different regions was investigated on the basis of the number fraction of spherical particles (DR <0.1, referred to as "NFS") as a function of the averaged RH, which was calculated along 3-day backward trajectories (Figure 8). The dataset period when intensive precipitation (>20 mm/hr) occurred along the trajectories was removed. The averaged RH of air masses from Regions III and IV were relatively high (>70%) because of their longer stagnancy in the marine area. For particles with 1.0 < Dp < 1.5 μm (Figure 8a), the NFS was positively correlated with the RH for particles from all origins. This phenomenon can be explained because of coexistence of hygroscopic masses such as sulfate and nitrate. About 70% of particles were spherical in the air mass from Region I, and this figure increased to 89% at RH = 76%. In the air masses from Region II, 62% of particles were spherical at RH = 45% and this increased to 72% at RH = 82%. For particles with 1.5 < Dp < 2.0 μm (Figure 8b), the overall NFS decreased for particles from all origins. The positive correlation between NFS and RH did not change when the air mass came from Region I; however, the tendency for the value to increase disappeared when the air masses came from Region II, implying that particles from Region II were less hygroscopic than those from Region I. The chemical analysis indicated that the mass fraction of water-soluble matter (WSM = SO_4^{2-} + NO_3^- + WSOCs + NH_4^+, Figure 9a) from Region II was the smallest (39.7%), although the mass concentration of $PM_{2.5}$ (Figure 9b), SO_4^{2-} (Figure 9c), and NO_3^- (Figure 9d) was statistically high with median values of 21.6, 4.2, and 1.5 μg/m^3, respectively. The missing part in mass balance was likely to be related to dust species, because the hygroscopic

Atmos. Chem. Phys. Discuss., doi:10.5194/acp-2015-904, 2016
Manuscript under review for journal Atmos. Chem. Phys.
Published: 26 January 2016

Atmospheric Chemistry and Physics Discussions

growth of aerosol particles was very weak when small dust particles were present (Pan *et al.,* 2009). For coarse mode particles (Figure 8c) from Region II, the NFS was about 32%, irrespective of RH; however, the NFS from Region I was still very sensitive to the variation in RH, which suggested that the aerosol particles were related to sea salt. The high NFS value (50 - 90%) and clear RH-dependency for aerosol particles from Region IV (blue circles in Figure 8) also indicated a great impact of sea salt (as shown by the 5-day backward trajectories in Figure 7e). The Acidity (ΔH, defined as the change of molar concentration of hydrogen ion after sampled particles dissolved into the extracting solution) of polluted particle normally decreased if alkaline substances (Ca^{2+}, Mg^{2+} etc.) were surplus. When the air mass came from Region II, about 30% of the data were found to have negative acidity value (shown in supplementary material), also implying that the particles consisted of crustal substances. However, ΔH values of particles from other regions were normally positive. This difference also partially explained the weaker hygroscopicity of particle from Region II than other regions.

5 Conclusions

In this study, we conducted continuous observations of the polarization properties and chemical composition of aerosol particles in Kyushu over a one-year period, using a Polarization Optical Particle Counter (POPC) and Aerosol Chemical Speciation Analyzer (ACSA-12). The conclusions were as follows: (1) POPC could objectively identify anthropogenic pollutants, mineral dust, and sea salt particles from their distinct depolarization ratio-size-volume relationships. It was concluded that the depolarization ratio of 0.1 is a reliable threshold that can be used to classify the sphericity/non-sphericity of supermicron particles. Based on this criterion, we found that long-range-transport dust and mixed aerosols were mainly responsible for substandard air quality days in western Japan during spring 2014. (2) Spherical particles in the coarse mode in summer were mostly due to the impact of sea salt at high RH conditions, whereas particles were normally non-spherical, in particular when the air masses came from the Asian continent. (3) The number fraction of spherical particles (NFS) decreased as particle size increased. When the particles came from the Asian continent, the correlation between NFS and RH was not significant because of the existence of dust particles. The positive correlation between NFS and RH for the supermicron particles implied a great impact of sea salt when the air mass originated from Region I. (4) Local emissions were partially responsible for the occurrence of substandard air quality days in Kyushu, although the LRT of anthropogenic pollutants was significant.

Atmos. Chem. Phys. Discuss., doi:10.5194/acp-2015-904, 2016
Manuscript under review for journal Atmos. Chem. Phys.
Published: 26 January 2016

Atmospheric Chemistry and Physics Discussions

Acknowledgments

This work was supported by a Grant-in-Aid for Scientific Research (25220101) from the Japan Society for the Promotion of Science (JSPS). For request POPC data for scientific research purposes, please contact with Prof. Itsushi Uno at Kyushu University via email (uno@riam.kyushu-u.ac.jp).

Atmos. Chem. Phys. Discuss., doi:10.5194/acp-2015-904, 2016
Manuscript under review for journal Atmos. Chem. Phys.
Published: 26 January 2016

Atmospheric Chemistry and Physics Discussions

References

Allen H. M., Draper D. C., Ayres B. R., Ault A., Bondy A., Takahama S., Modini R. L., Baumann K., Edgerton E., Knote C. Influence of crustal dust and sea spray supermicron particle concentrations and acidity on inorganic NO 3− aerosol during the 2013 Southern Oxidant and Aerosol Study. Atmospheric Chemistry and Physics. 15(18):10669-85, 2015.

Dubovik O., Sinyuk A., Lapyonok T., Holben B. N., Mishchenko M., Yang P., Eck T. F., Volten H., Munoz O., Veihelmann B. Application of spheroid models to account for aerosol particle nonsphericity in remote sensing of desert dust. Journal of Geophysical Research: Atmospheres (1984–2012). 111(D11), 2006.

Fu H., Zhang M., Li W., Chen J., Wang L., Quan X., Wang W. Morphology, composition and mixing state of individual carbonaceous aerosol in urban Shanghai. Atmospheric Chemistry and Physics. 12(2):693-707, 2012.

Itahashi S., Yumimoto K., Uno I., Eguchi K., Takemura T., Hara Y., Shimizu A., Sugimoto N., Liu Z. Structure of dust and air pollutant outflow over East Asia in the spring. Geophysical Research Letters. 37(20), 2010.

Kaneyasu N., Yamamoto S., Sato K., Takami A., Hayashi M., Hara K., Kawamoto K., Okuda T., Hatakeyama S. Impact of long-range transport of aerosols on the PM2.5 composition at a major metropolitan area in the northern Kyushu area of Japan. Atmospheric Environment.416-25, 2014.

Kimoto H., Ueda A., Tsujimoto K., Mitani Y., Toyazaki Y., Kimoto T. Development of a Continuous Dichotomous Aerosol Chemical Speciation Analyzer. Clean Technology. 23:49-52, 2013.

Kobayashi H., Hayashi M., Shiraishi K., Nakura Y., Enomoto T., Miura K., Takahashi H., Igarashi Y., Naoe H., Kaneyasu N. Development of a polarization optical particle counter capable of aerosol type classification. Atmospheric Environment.486-92, 2014.

Koehler K. A., Kreidenweis S. M., DeMott P. J., Petters M. D., Prenni A. J., Carrico C. M. Hygroscopicity and cloud droplet activation of mineral dust aerosol. Geophysical Research Letters. 36(8), 2009.

Kurokawa J., Ohara T., Morikawa T., Hanayama S., Janssens-Maenhout G., Fukui T., Kawashima K., Akimoto H. Emissions of air pollutants and greenhouse gases over Asian regions during 2000–2008: Regional Emission inventory in ASia (REAS) version 2. Atmospheric Chemistry and Physics. 13(21):11019-58, 2013.

Li W. J., Shao L. Y. Observation of nitrate coatings on atmospheric mineral dust particles. Atmospheric Chemistry and Physics. 9(6):1863-71, 2009.

Li W. J., Zhang D. Z., Shao L. Y., Zhou S. Z., Wang W. X. Individual particle analysis of aerosols collected under haze and non-haze conditions at a high-elevation mountain site in the North China plain. Atmospheric Chemistry and Physics. 11(22):11733-44, 2011.

Pan X. L., Uno I., Hara Y., Kuribayashi M., Kobayashi H., Sugimoto N., Yamamoto S., Shimohara T., Wang Z. Observation of the simultaneous transport of Asian mineral dust aerosols with anthropogenic pollutants using a polarization optical particle counter (POPC) during a long-lasting dust event in late spring 2014. Geophysical Research Letters.2014GL062491, 2015. 10.1002/2014GL062491

Pan X. L., Yan P., Tang J., Ma J. Z., Wang Z. F., Gbaguidi A., Sun Y. L. Observational study of influence of aerosol hygroscopic growth on scattering coefficient over rural area near Beijing mega-city. Atmospheric Chemistry and Physics. 9(19):7519-30, 2009.

Shimizu A., Sugimoto N., Matsui I., Arao K., Uno I., Murayama T., Kagawa N., Aoki K., Uchiyama A., Yamazaki A. Continuous observations of Asian dust and other aerosols by

polarization lidars in China and Japan during ACE-Asia. Journal of Geophysical Research: Atmospheres (1984–2012). 109(D19), 2004.

Sugimoto N., Huang Z. Lidar methods for observing mineral dust. Journal of Meteorological Research. 28(2):173-84, 2014.

Sugimoto N., Matsui I., Shimizu A., Uno I., Asai K., Endoh T., Nakajima T. Observation of dust and anthropogenic aerosol plumes in the northwest Pacific with a two-wavelength polarization lidar on board the research vessel Mirai. Geophysical Research Letters. 29(19):7-1-7-4, 2002.

Sugimoto N., Nishizawa T., Shimizu A., Matsui I., Kobayashi H. Detection of internally mixed Asian dust with air pollution Aerosols using a polarization optical particle counter and a polarization-sensitive two-wavelength lidar. Journal of Quantitative Spectroscopy and Radiative Transfer. 150:107-13, 2015. 10.1016/j.jqsrt.2014.08.003

Sullivan R. C., Moore M. J. K., Petters M. D., Kreidenweis S. M., Roberts G. C., Prather K. A. Effect of chemical mixing state on the hygroscopicity and cloud nucleation properties of calcium mineral dust particles. Atmospheric Chemistry and Physics. 9(10):3303-16, 2009.

Tobo Y., Zhang D., Matsuki A., Iwasaka Y. Asian dust particles converted into aqueous droplets under remote marine atmospheric conditions. Proceedings of the National Academy of Sciences. 107(42):17905-10, 2010.

Uno I., Eguchi K., Yumimoto K., Takemura T., Shimizu A., Uematsu M., Liu Z., Wang Z., Hara Y., Sugimoto N. Asian dust transported one full circuit around the globe. Nature Geoscience. 2(8):557-60, 2009.

Wang Z., Akimoto H., Uno I. Neutralization of soil aerosol and its impact on the distribution of acid rain over east Asia: Observations and model results. Journal of Geophysical Research: Atmospheres (1984–2012). 107(D19):ACH 6-1-ACH 6-12, 2002.

Winker D. M., Vaughan M. A., Omar A., Hu Y., Powell K. A., Liu Z., Hunt W. H., Young S. A. Overview of the CALIPSO mission and CALIOP data processing algorithms. Journal of Atmospheric and Oceanic Technology. 26(11):2310-23, 2009.

Wise M. E., Semeniuk T. A., Bruintjes R., Martin S. T., Russell L. M., Buseck P. R. Hygroscopic behavior of NaCl-bearing natural aerosol particles using environmental transmission electron microscopy. Journal of Geophysical Research: Atmospheres (1984–2012). 112(D10), 2007.

Yumimoto K., Eguchi K., Uno I., Takemura T., Liu Z., Shimizu A., Sugimoto N. An elevated large-scale dust veil from the Taklimakan Desert: Intercontinental transport and three-dimensional structure as captured by CALIPSO and regional and global models. Atmospheric Chemistry and Physics. 9(21):8545-58, 2009.

Zhang D., Iwasaka Y., Matsuki A., Ueno K., Matsuzaki T. Coarse and accumulation mode particles associated with Asian dust in southwestern Japan. Atmospheric Environment. 40(7):1205-15, 2006.

Zhang D., Iwasaka Y., Shi G., Zang J., Hu M., Li C. Separated status of the natural dust plume and polluted air masses in an Asian dust storm event at coastal areas of China. Journal of Geophysical Research: Atmospheres (1984–2012). 110(D6), 2005.

Atmos. Chem. Phys. Discuss., doi:10.5194/acp-2015-904, 2016
Manuscript under review for journal Atmos. Chem. Phys.
Published: 26 January 2016

Atmospheric Chemistry and Physics Discussions

1

Atmos. Chem. Phys. Discuss., doi:10.5194/acp-2015-904, 2016
Manuscript under review for journal Atmos. Chem. Phys.
Published: 26 January 2016

Atmospheric Chemistry and Physics Discussions

Table 1 Statistics for the mass concentrations of $PM_{2.5}$, $PM_{2.5-10}$, fSO_4^{2-}, fNO_3^-, and cNO_3^- for three typical types of aerosol. The numbers in brackets represent total hours for episodes of specific types of aerosol.

Aerosol types		**$PM_{2.5}$**	**$PM_{2.5-10}$**	**fSO_4^{2-}**	**fNO_3^-**	**cNO_3^-**
Anthropogenic pollutant (n = 12)	*Max.*	74.5	16.9	19.3	15.2	3.5
	Min.	52.4	10.8	15.3	10.0	2.4
	Avg. SD.	63.4 ± 7.0	12.9 ± 1.9	17.2 ± 1.2	11.5 ± 1.4	2.8 ± 0.3
Mineral dust (n = 8)	*Max.*	35.8	81.3	3.0	1.9	2.7
	Min.	23.8	51.4	2.4	0.9	1.4
	Avg. SD.	27.5 ± 4.7	62.9 ± 12.6	2.7 ± 0.2	1.4 ± 0.4	1.8 ± 0.6
Sea salt (n = 13)	*Max.*	13.2	35.8	3.0	1.0	1.0
	Min.	0.2	0.1	0.1	0.2	0.1
	Avg. SD.	6.6 ± 3.2	9.7 ± 7.7	1.3 ± 0.8	0.5 ± 0.2	0.4 ± 0.2

Atmos. Chem. Phys. Discuss., doi:10.5194/acp-2015-904, 2016
Manuscript under review for journal Atmos. Chem. Phys.
Published: 26 January 2016

Atmospheric Chemistry and Physics Discussions

List of Figures

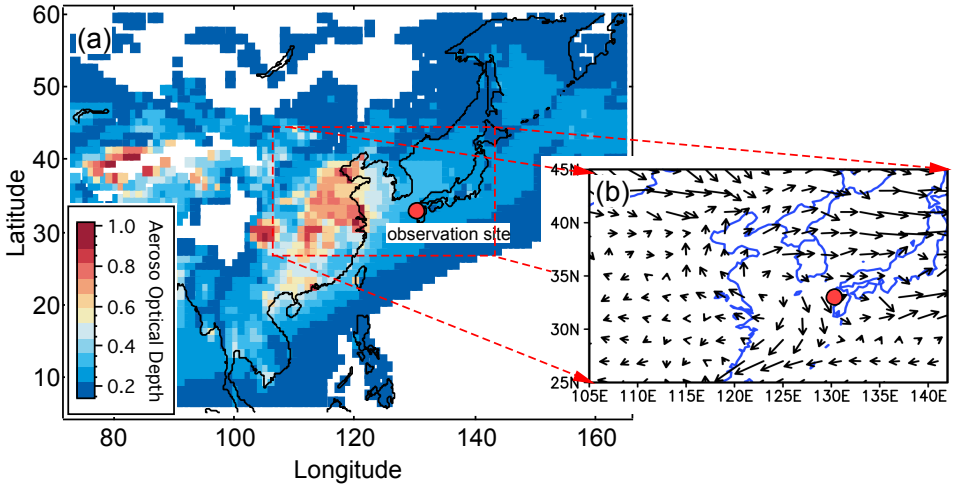

Figure 1 Geographic location of the observation site. (a) Spatial distribution of aerosol optical depth (AOD) at 550 nm by Moderate-resolution Imaging Spectroradiometer (MODIS) in East Asia and (b) the averaged surface wind field in Spring (MAM).

Atmos. Chem. Phys. Discuss., doi:10.5194/acp-2015-904, 2016
Manuscript under review for journal Atmos. Chem. Phys.
Published: 26 January 2016

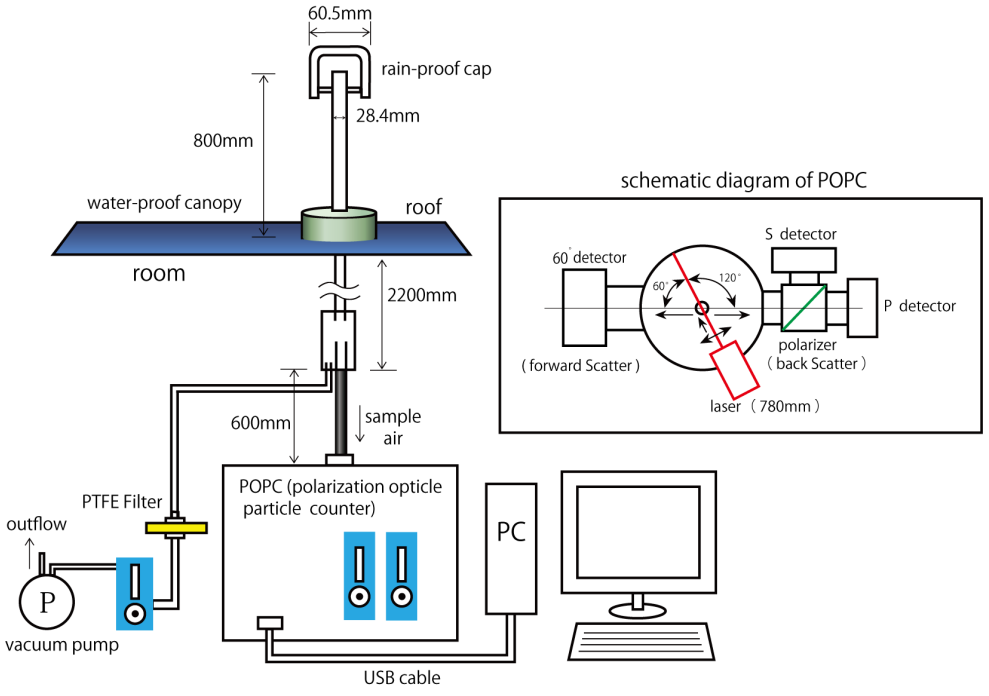

Figure 2 The layout of the instrument and schematic diagram of the polarization optical particle counter (POPC).

Atmos. Chem. Phys. Discuss., doi:10.5194/acp-2015-904, 2016
Manuscript under review for journal Atmos. Chem. Phys.
Published: 26 January 2016

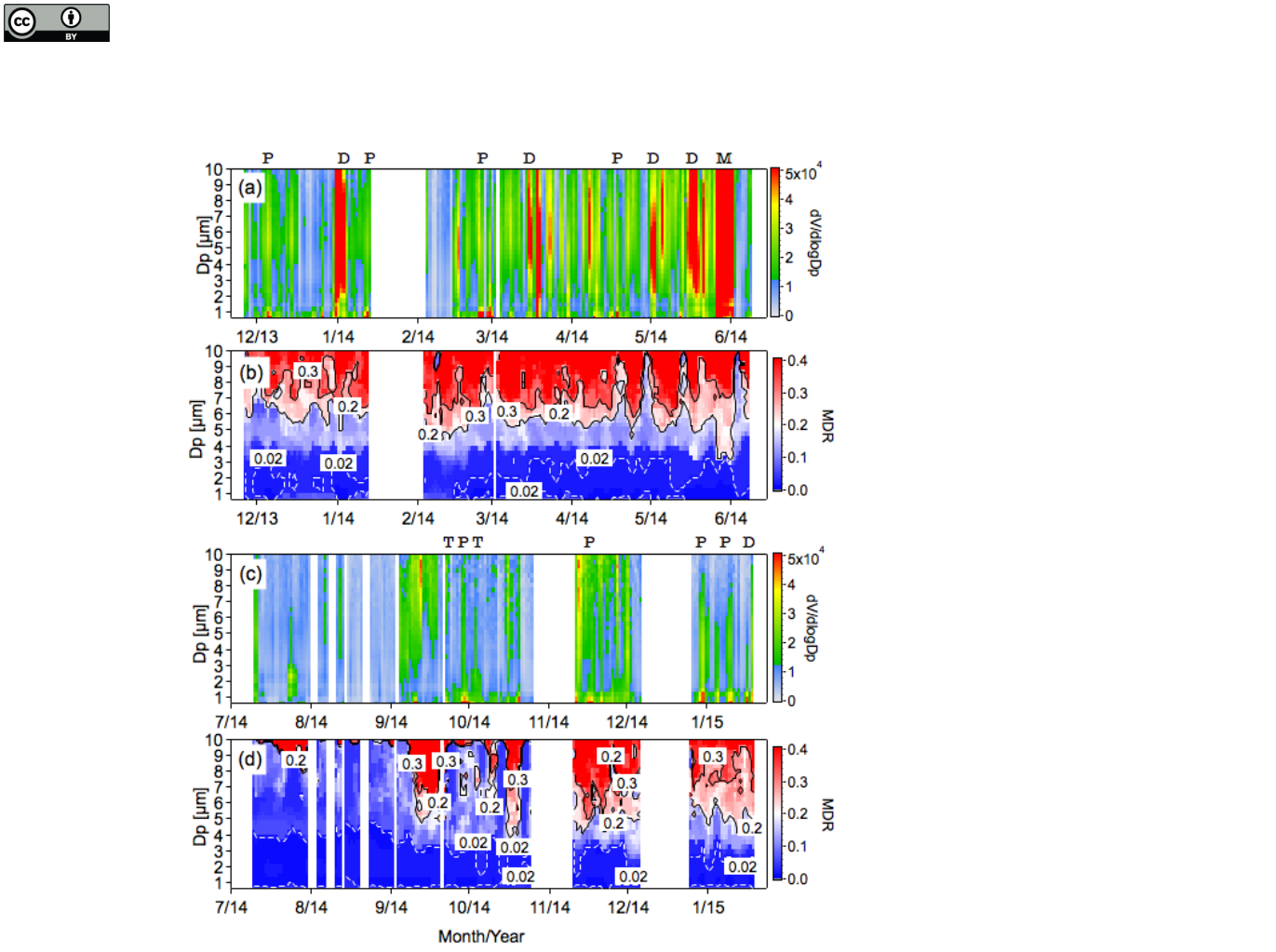

Figure 3 Time series of volume size distributions (a, c) and mode depolarization ratios (MDRs) (b, d) of ambient particles at the observation site. The letters "P," "D", "T" and "M" at the top of figure indicate pollution, dust, Typhoon and mixed type dominated cases.

Atmos. Chem. Phys. Discuss., doi:10.5194/acp-2015-904, 2016
Manuscript under review for journal Atmos. Chem. Phys.
Published: 26 January 2016

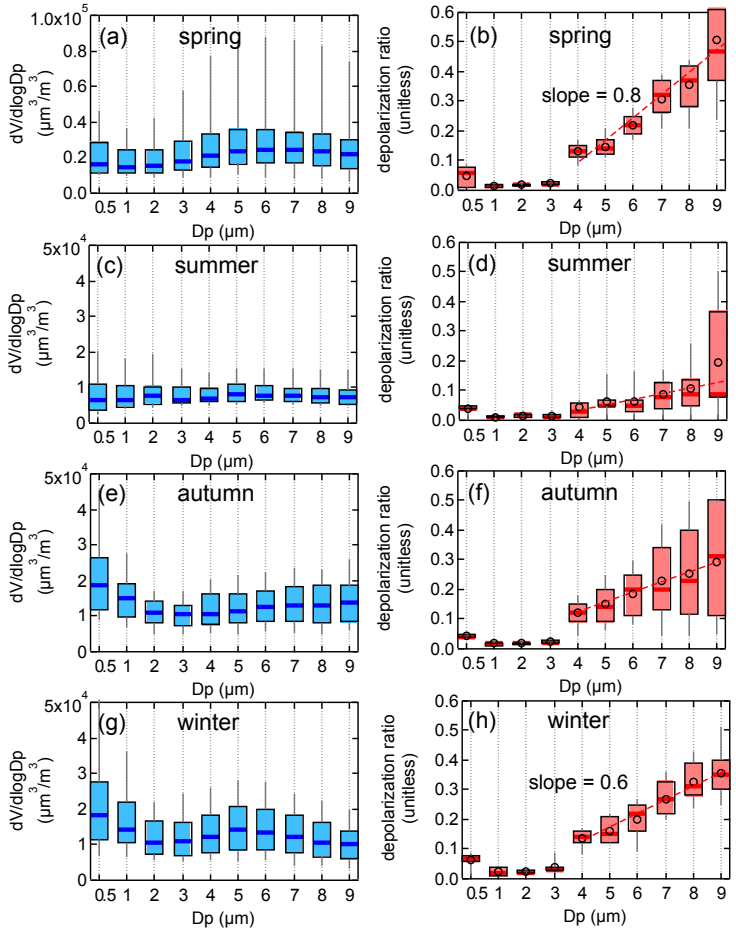

Figure 4 Volume size distribution (a, c, e, g) and size-dependent depolarization ratio (DR) (b, d, f, h) of aerosols in Kyushu in Spring (MAM), Summer (JJA), Autumn (SON), Winter (DJF). The box and whiskers in the plot represent the 10th, 25th, 75th, 90th percentiles and median values, and the black circles in the right panel are the mean values, respectively.

Atmos. Chem. Phys. Discuss., doi:10.5194/acp-2015-904, 2016
Manuscript under review for journal Atmos. Chem. Phys.
Published: 26 January 2016

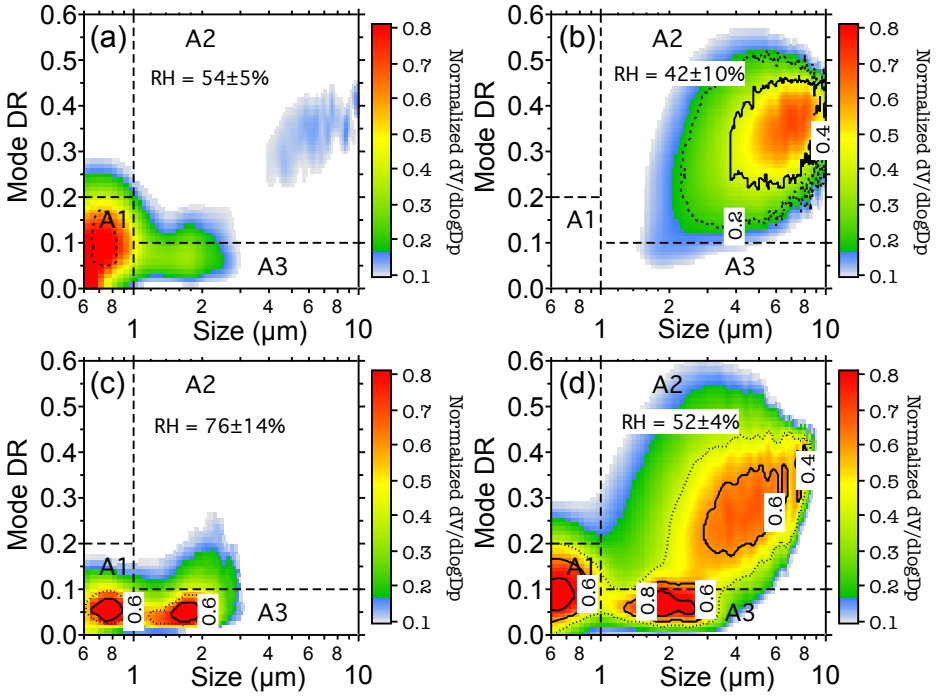

Figure 5 Variation in the mode depolarization ratio as a function of size for (a) anthropogenic pollution, (b) mineral dust, (c) sea salt, and (d) mixed particle types. Colors represent normalized volume concentrations (maximum value = 1).

Atmos. Chem. Phys. Discuss., doi:10.5194/acp-2015-904, 2016
Manuscript under review for journal Atmos. Chem. Phys.
Published: 26 January 2016

Atmospheric Chemistry and Physics Discussions

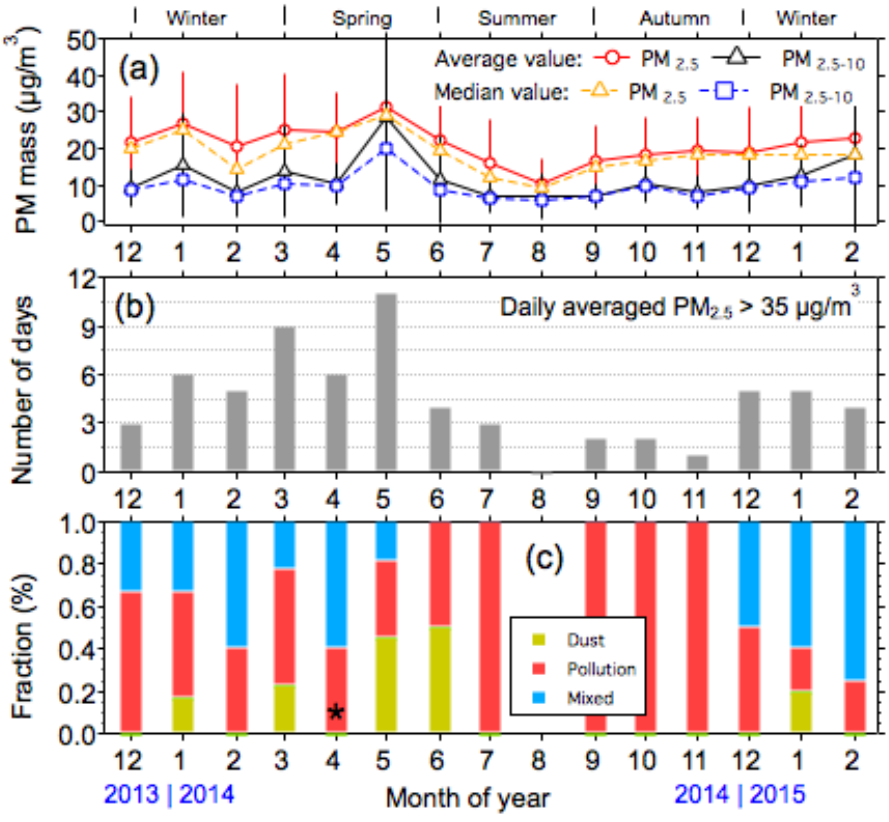

Figure 6 (a) The monthly mean and median values of mass concentrations of $PM_{2.5}$ and $PM_{2.5-10}$, (b) number of days, with daily averaged mass concentrations of $PM_{2.5}$ exceeding 35 μg/m^3 (the National Ambient Air Quality Standard (NAAQS) of $PM_{2.5}$ in Japan), and (c) the relative monthly contribution of different aerosol types. The asterisk symbol highlights that no dust incursions were observed during April 2014 in the Kyushu area.

Atmos. Chem. Phys. Discuss., doi:10.5194/acp-2015-904, 2016
Manuscript under review for journal Atmos. Chem. Phys.
Published: 26 January 2016

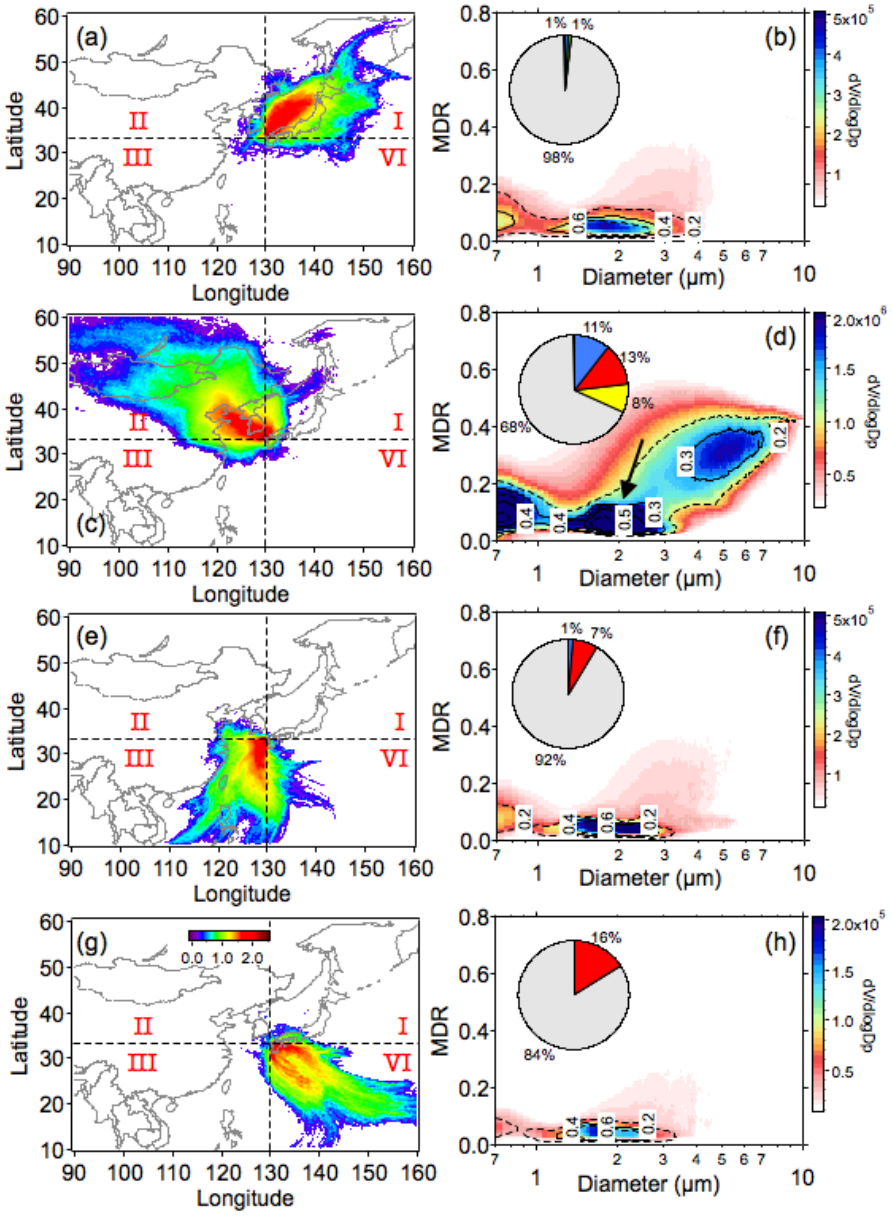

Figure 7 Air masses originating from Region I (a), Region II (c), Region III (e) and Region IV (g). The color scale represents the logarithm of the total number of trajectories that passed through the mixing layer of the target grid. The corresponding size-resolved depolarization characteristics of transported particles are shown in b, d, f and h. The colors gray, red, yellow, and blue in the pie charts indicate the fraction of days, which met the air quality standard and substandard air quality days caused by anthropogenic pollution, dust, or mixed pollution, respectively.

Atmos. Chem. Phys. Discuss., doi:10.5194/acp-2015-904, 2016
Manuscript under review for journal Atmos. Chem. Phys.
Published: 26 January 2016

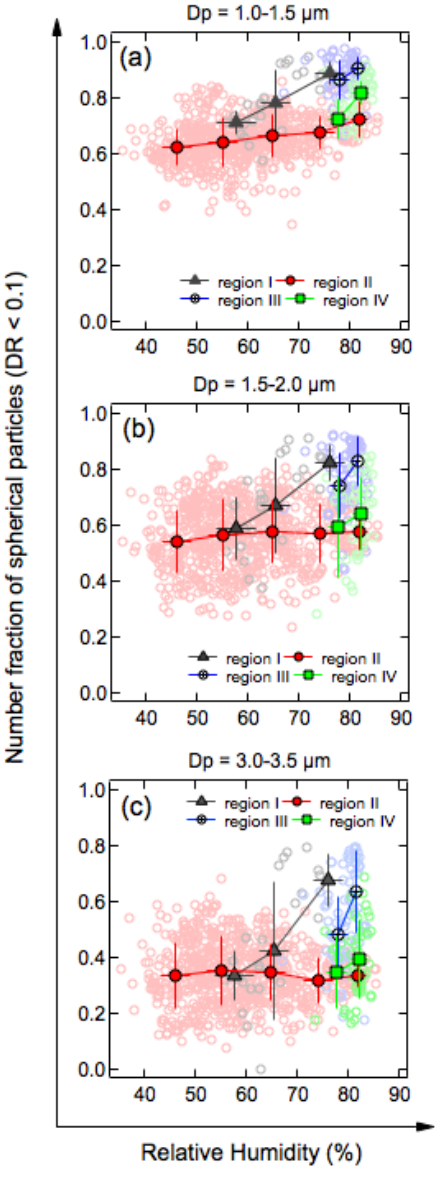

Figure 8 Number fractions of spherical particles as a function of relative humidity (RH) for the size ranges (a) 1.0-1.5 μm, (b) 1.5-2.0 μm, and (c) 3.0-3.5 μm.

Atmos. Chem. Phys. Discuss., doi:10.5194/acp-2015-904, 2016
Manuscript under review for journal Atmos. Chem. Phys.
Published: 26 January 2016

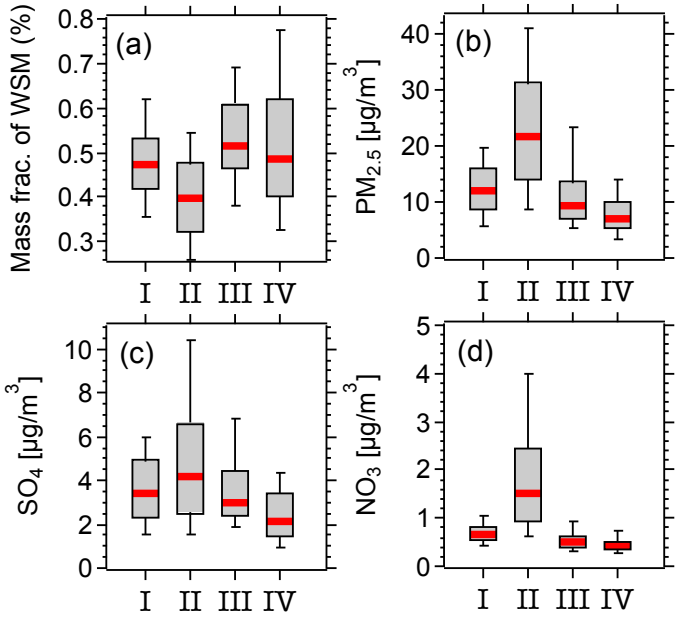

Figure 9 Box and whisker plots of the mass fraction of (a) water soluble matter (SO_4^{2-} + NO_3^- + WSOCs + $NH4^+$), (b) $PM_{2.5}$, (c) SO_4^{2-} and (d) NO_3^-, ions in the fine mode for the air masses from Region I, II, III and IV. The mass concentration of $NH4^+$ was estimated on the basis of the correlation (r^2 = 0.63) between [SO_4^{2-} + NO_3^-] and [$NH4^+$] from the analysis of filter samples using ion chromatography in Kyushu.